

## Original Paper

# Inhibition of Lithium Sensitive Orai1/STIM1 Expression and Store Operated $\text{Ca}^{2+}$ Entry in Chorea-Acanthocytosis Neurons by NF- $\kappa$ B Inhibitor Wogonin

Basma Sukkar<sup>a</sup> Stefan Hauser<sup>b</sup> Lisann Pelzl<sup>a</sup> Zohreh Hosseinzadeh<sup>c</sup>  
Itishri Sahu<sup>a</sup> Tamer al-Maghout<sup>a</sup> Abdulla Al Mamun Bhuyan<sup>a</sup>  
Nefeli Zacharopoulou<sup>d</sup> Christos Stournaras<sup>d</sup> Ludger Schöls<sup>b,e</sup> Florian Lang<sup>f</sup>

<sup>a</sup>Department of Internal Medicine III, University of Tübingen, Tübingen, <sup>b</sup>German Center for Neurodegenerative Diseases, Tübingen, <sup>c</sup>Technische Universität Dresden Center for Molecular and Cellular Bioengineering (CMCB), Dresden, Germany, <sup>d</sup>Department of Biochemistry, University of Crete Medical School, Heraklion, Greece, <sup>e</sup>Department of Neurology and Hertie Institute for Clinical Brain Research, University of Tübingen, Tübingen, <sup>f</sup>Department of Vegetative and Clinical Physiology, University of Tübingen, Tübingen, Germany

## Key Words

Chorein • Neurons • Lithium • NF $\kappa$ B • Orai1 • SOCE

## Abstract

**Background/Aims:** The neurodegenerative disease Chorea-Acanthocytosis (ChAc) is caused by loss-of-function-mutations of the chorein-encoding gene VPS13A. In ChAc neurons transcript levels and protein abundance of  $\text{Ca}^{2+}$  release activated channel moiety (CRAC) Orai1 as well as its regulator STIM1/2 are decreased, resulting in blunted store operated  $\text{Ca}^{2+}$ -entry (SOCE) and enhanced suicidal cell death. SOCE is up-regulated and cell death decreased by lithium. The effects of lithium are paralleled by upregulation of serum & glucocorticoid inducible kinase SGK1 and abrogated by pharmacological SGK1 inhibition. In other cell types SGK1 has been shown to be partially effective by upregulation of NF $\kappa$ B, a transcription factor stimulating the expression of Orai1 and STIM. The present study explored whether pharmacological inhibition of NF $\kappa$ B interferes with Orai1/STIM1/2 expression and SOCE and their upregulation by lithium in ChAc neurons. **Methods:** Cortical neurons were differentiated from induced pluripotent stem cells generated from fibroblasts of ChAc patients and healthy volunteers. Orai1 and STIM1 transcript levels and protein abundance were estimated from qRT-PCR and Western blotting, respectively, cytosolic  $\text{Ca}^{2+}$ -activity ( $[\text{Ca}^{2+}]_i$ ) from Fura-2-fluorescence, SOCE from increase of  $[\text{Ca}^{2+}]_i$  following  $\text{Ca}^{2+}$  re-addition after  $\text{Ca}^{2+}$ -store depletion with sarco-endoplasmic  $\text{Ca}^{2+}$ -ATPase inhibitor thapsigargin (1  $\mu\text{M}$ ), as well as CRAC current utilizing whole cell patch clamp

B. Sukkar and S. Hauser contributed equally to this work and thus share first authorship.

Prof. Dr. Florian Lang

Institut für Vegetative und Klinische Physiologie, Universität Tübingen  
Wilhelmstr. 56, D-72074 Tübingen (Germany)  
Tel. +49 7071 29 72194, Fax +49 7071 29 5618, E-Mail [florian.lang@uni-tuebingen.de](mailto:florian.lang@uni-tuebingen.de)

recording. **Results:** Orai1 and STIM1 transcript levels and protein abundance as well as SOCE and CRAC current were significantly enhanced by lithium treatment (2 mM, 24 hours). These effects were reversed by NFκB inhibitor wogonin (50 μM). **Conclusion:** The stimulation of expression and function of Orai1/STIM1/2 by lithium in ChAc neurons are disrupted by pharmacological NFκB inhibition.

© 2018 The Author(s)  
Published by S. Karger AG, Basel

## Introduction

Chorein binds to and supports activation of phosphoinositide-3-kinase (PI3K)-p85-subunit thus participating in the regulation of actin polymerization and cell survival [1-4]. Loss-of-function-mutations of the chorein encoding gene VPS13A (vacuolar protein sorting-associated protein 13A) result in chorea-acanthocytosis (ChAc) [5, 6], a neurodegenerative disease with hyperkinetic movements, epilepsy, impaired cognitive functions, myopathy, and erythrocyte acanthocytosis [5, 7-9]. The progressive neurodegeneration eventually leads to severe disability and early death [9]. Erythrocyte shape changes [10], neuronal apoptosis [11] and altered behaviour [11] are similarly observed in gene targeted mice lacking functional chorein.

Chorein expression is observed in a wide variety of tissues and across a wide range of cell types [12-14]: Chorein-sensitive functions include dopamine release [15], platelet activation [14], cytoskeletal architecture [16], endothelial cell stiffness [13], as well as survival of tumour cells [3], neurons and skeletal muscle cells [5, 17].

Cell survival and cell death are sensitive to alterations of cytosolic  $Ca^{2+}$  activity ( $[Ca^{2+}]_i$ ) [18, 19].  $[Ca^{2+}]_i$  could be increased by  $Ca^{2+}$  release from intracellular stores with subsequent store-operated  $Ca^{2+}$  entry (SOCE) through the pore-forming  $Ca^{2+}$  channel subunits Orai1, Orai2 and/or Orai3 [20]. The Orai isoforms are activated following store depletion by the  $Ca^{2+}$  sensing proteins STIM1 and/or STIM2 [21-23]. Orai1 and SOCE are up-regulated by PI3K dependent signaling and thus sensitive to chorein [24]. Stimulators of Orai1 expression and SOCE include lithium [25-27], which may slow neurodegeneration [28-30].

Orai1 expression is up-regulated by serum & glucocorticoid inducible kinase SGK1 [31, 32] and the effect of lithium in ChAc neurons is reversed in the presence of SGK1 inhibitor GSK650394 [27]. SGK1 is partially effective by NFκB dependent up-regulation of Orai1 expression and by inhibition of Nedd4-2 triggered degradation of Orai1 protein [31, 32]. As chorein deficiency impairs activation of PI3K [1-3], it should interfere with PI3K/SGK1/NFκB dependent Orai1 upregulation. The observed signaling contributes to the anti-apoptotic effect of PI3K which confers survival of a wide variety of cells including cancer cells [33-36] and neurons [37-40].

The present study explored whether the effect of lithium on neuronal Orai1 expression and SOCE in ChAc neurons requires functional NFκB. To this end, skin fibroblasts from ChAc patients were reprogrammed and differentiated to neurons and Orai1/STIM1/STIM2 transcript levels, Orai1/STIM1/STIM2 protein abundance, SOCE and CRAC currents determined without or with prior lithium treatment in the absence or presence of NFκB inhibitor wogonin.

## Materials and Methods

### Generation of iPSCs

The study has been approved by the Ethical Commission of the University of Tübingen (598/2011). Informed consent was obtained from all participants and/or their legal guardian/s. Human dermal fibroblasts were isolated from ChAc patients (n = 3) and healthy volunteers (n = 3). Dermal fibroblasts were cultivated in fibroblast medium, consisting of DMEM (Biochrom, Berlin, Germany) supplemented with 10% fetal calf serum (FCS, Life technologies, Thermo Fisher Scientific, Waltham, Massachusetts) and 1% L-Glutamine (Biochrom). Induced pluripotent stem cells (iPSCs) were generated following a protocol

published previously [41], with minor modifications. In brief,  $1 \times 10^5$  fibroblasts were electroporated (Nucleofector 2D, Lonza) with a total of 1  $\mu$ g per plasmid carrying the sequences for hOCT4, hSOX2, hKLF4, hL-MYC and hLIN28. After cultivation in fibroblast medium for 1 day, 2 ng/ml FGF-2 (Peprotech) was supplemented to the medium. From day 3 on, cells were cultivated in Essential 8 (E8) medium containing 100  $\mu$ M NaB (Sigma-Aldrich). The iPSC colonies were picked manually after 3 – 4 weeks and further expanded in Matrigel coated 6-well plates. At passage 7 – 10, iPSCs were characterized and frozen in E8 medium supplemented with 40% KOSR (Thermo Fisher Scientific), 10% DMSO (Sigma-Aldrich), and 1  $\mu$ M Y-27632 (Selleckchem, Munich, Germany). Characterization of generated iPSCs included genomic validation via exclusion of plasmid-integration, SNParray analysis for genetic integrity, and resequencing of mutation site, as well as functional validation via confirmation of expression of pluripotency marker, and verification of the *in vitro* differentiation potential as described previously [42]. The opportunity to apply iPSC-derived neurons to model neurological disorders is a powerful tool to identify disease-relevant alterations in patient-specific neuronal cell types (reviewed in: [43]). A careful characterization of generated iPSCs as well as the establishment of a robust and reliable protocol to generate neurons is essential to provide consistent phenotypes. Additionally, using multiple patient and control cell lines is crucial to confirm the identified cellular phenotypes. In the present study we addressed these points by genomic and functional validation of all generated iPSCs, applying a standardized neuronal differentiation protocol yielding  $\beta$ -III-tubulin/CTIP-2 positive neurons as well as verifying the observed phenotypes in three independent patient lines.

#### Neuronal differentiation and treatment of iPSCs

Cortical neurons were generated as described previously [44]. Briefly, neural induction of iPSCs was achieved by addition of dual SMAD inhibitors (10  $\mu$ M SB431542 (Sigma-Aldrich) and 500 nM LDN-193189 (Sigma-Aldrich)) to 3N medium. Cells were collected at day 10 and further expanded by cultivation in 3N medium supplemented with 20 ng/ml FGF-2 for 2 days. From day 12 on, cells were cultivated in 3N medium with medium change every other day. Cell cultures were passaged at day 27 and replated appropriately for the specific assay (RNA/Protein isolation:  $5 \times 10^5$  cells per  $\text{cm}^2$ ; FACS analysis:  $2.5 \times 10^5$  per  $\text{cm}^2$ ;  $\text{Ca}^{2+}$  measurements:  $5 \times 10^4$  per  $\text{cm}^2$ ). Where indicated, 2 mM lithium (Sigma-Aldrich) and/or 50  $\mu$ M wogonin (Sigma-Aldrich) was added to the medium 24 hours prior to measurements. Analysis was performed between day 37 and 41.

#### Quantitative PCR

Transcript levels of Orai1, STIM1, STIM2 and house-keeping GAPDH were determined by RT-PCR as described previously [24, 45]. Total RNA was extracted in TriFast (Peqlab, Erlangen, Germany) according to the manufacturer's instructions. After DNase digestion reverse transcription of 2  $\mu$ g RNA was performed using GoScript™ Reverse Transcription System (Promega, Hilden, Germany) according to the manufacturer's protocol. Real-time polymerase chain reaction (RT-PCR) amplification of the respective genes were set up in a total volume of 20  $\mu$ l using 40 ng of cDNA, 500 nM forward and reverse primer and 2x GoTaq® qPCR Master Mix (Promega, Hilden, Germany) according to the manufacturer's protocol. Cycling conditions were as follows: Initial denaturation at 95°C for 2 minutes, followed by 40 cycles of 95°C for 15 seconds, 55°C for 15 seconds and 68°C for 20 seconds. For amplification the following primers were used (5'→3' orientation):

GAPDH:

fw: TGAGTACGTCGTGGAGTCCAC;

rev: GTGCTAAGCAGTTGGTGGTG

Orai1:

fw: CGTATCTAGAATGCATCCGAGCC;

rev: CAGCCACTATGCCTAGGTCGACTAGC

STIM1:

fw: CCTCGGTACCATCCATGTTGTAGCA

rev: GCGAAAGCTTACGCTAAAATGGTGTCT

STIM2:

fw: CAAGTTGCCCTGCGCTTTAT

rev: ATTCACCTTTGCACGCACCG

Specificity of PCR products was confirmed by analysis of a melting curve. Real-time PCR amplifications were performed on a CFX96 Real-Time System (Bio-Rad, Munich, Germany) and all experiments were done in duplicate. The house-keeping gene GAPDH (Glyceraldehyde 3-phosphate dehydrogenase) was amplified to standardize the amount of sample RNA.

## Western Blotting

Protein abundance of Orai1, STIM1/2 and GAPDH was determined by Western blotting as described previously [24, 45]. To this end, cells were centrifuged for 5 minutes at 240 g and 4°C. The pellet was washed twice with ice cold PBS and suspended in 40 µl ice-cold RIPA lysis buffer (Thermo Fisher Scientific, USA) containing Halt Protease and Halt Phosphatase Inhibitor Cocktail (Thermo Fisher Scientific, USA). Protein concentration was determined using the Bradford assay (BioRad, München, Germany). 100 µg of protein were solubilized in sample buffer at 95°C for 10 min. The proteins were separated by 10% SDS-PAGE in Glycine-Tris buffer and electro-transferred onto nitrocellulose membranes for 90 min. After blocking with 5% milk in TBST at room temperature for 1 h, the membranes were incubated with primary anti-ORAI1 antibody (1:1000, Proteintech), anti-STIM1 antibody (1:1000, Cell Signaling), anti-STIM2 antibody (1:1000, Cell Signaling) and anti-GAPDH antibody (1:1000, Cell Signaling) at 4°C overnight. After washing (TBST), the blots were incubated with secondary anti-rabbit antibody conjugated with horseradish peroxidase (1:2000, Cell Signaling) for 1 h at room temperature. Protein bands were detected after additional washes (TBST) with an ECL detection reagent (Amersham, Freiburg, Germany) and quantified with Quantity One Software (BioRad, München, Germany). To assign the right protein size we used Protein-Marker VI (Peqlab, Erlangen, Germany).

## Ca<sup>2+</sup> measurements

Fura-2 fluorescence was taken as a measure of cytosolic Ca<sup>2+</sup> concentration ([Ca<sup>2+</sup>]<sub>i</sub>), as described previously [24, 45]. For this purpose, cells were loaded with Fura-2/AM (2 µM, Invitrogen, Goettingen, Germany) for 20 min at 37°C. Cells were excited alternatively at 340 nm and 380 nm through an objective (Fluor 40×/1.30 oil) built in an inverted fluorescence microscope (Axiovert 100, Zeiss, Oberkochen, Germany). Emitted fluorescence intensity was recorded at 505 nm. Data were acquired using specialized computer software (Metafluor; Universal Imaging, Downingtown, USA). Cytosolic Ca<sup>2+</sup> activity was estimated from the 340 nm/380 nm ratio. SOCE was determined by extracellular Ca<sup>2+</sup> removal and subsequent Ca<sup>2+</sup> re-addition in the presence of thapsigargin (1 µM, Invitrogen). For quantification of Ca<sup>2+</sup> entry, the slope (delta ratio/s) and peak (delta ratio) were calculated following re-addition of Ca<sup>2+</sup>.

Experiments were performed with Ringer solution containing (in mM): 125 NaCl, 5 KCl, 1.2 MgSO<sub>4</sub>, 2 CaCl<sub>2</sub>, 2 Na<sub>2</sub>HPO<sub>4</sub>, 32 HEPES, 5 glucose, pH 7.4. To reach nominally Ca<sup>2+</sup>-free conditions, experiments were performed using Ca<sup>2+</sup>-free Ringer solution containing (in mM): 125 NaCl, 5 KCl, 1.2 MgSO<sub>4</sub>, 2 Na<sub>2</sub>HPO<sub>4</sub>, 32 HEPES, 0.5 EGTA, 5 glucose, pH 7.4.

## Patch clamp

Ca<sup>2+</sup> release activated channel (CRAC) currents (I<sub>CRAC</sub>) were determined by whole cell patch clamp recording at room temperature in voltage-clamp, fast whole cell mode. Cells were continuously superfused through a flow system inserted into the dish. The bath was grounded via a bridge filled with the external solution. Borosilicate glass pipettes (2- to 4-MΩ resistance; Harvard Apparatus, UK) manufactured by a microprocessor-driven DMZ puller (Zeitz, Augsburg, Germany), were used in combination with a MS314 electrical micromanipulator (MW, Märzhäuser, Wetzlar, Germany). The currents were recorded by an EPC-9 amplifier (Heka, Lambrecht, Germany) and analyzed with Pulse software (Heka) and an ITC-16 Interface (Instrutech, Port Washington, NY). Currents were recorded at an acquisition frequency of 10 kHz and 3 kHz low-pass filtered. The pipette solution contained (in mM/l): 35 NaCl, 120 CsCl, 10 HEPES/CsOH, 10 ethylene glycol tetraacetic acid (EGTA) and 0.04 inositol 1, 4,5-triphosphate (Ins(1, 4,5)P<sub>3</sub>, Enzo Life Sciences), pH 7.4. The external solution contained (in mM/l) 140 NaCl, 5 KCl, 10 CaCl<sub>2</sub>, 20 glucose, 10 HEPES/NaOH, pH 7.4 [46].

## Statistics

Data are expressed as arithmetic means ± SEM. Statistical analysis was made by unpaired t-test or Mann-Whitney test, as appropriate. p < 0.05 was considered as statistically significant.

## Results

ChAc neurons were incubated for 24 hours in the absence or presence of 2 mM lithium. The Orai1 and STIM1/2 mRNA abundance was subsequently determined using qRT-PCR. As displayed in Fig. 1, Orai1 and STIM1/2 transcript levels were in ChAc neurons significantly increased by treatment with 2 mM LiCl. The effect of lithium on Orai1 and STIM1/2 transcript levels was abrogated by additional treatment with the NFκB inhibitor wogonin (50 μM). In the presence of lithium and wogonin, the Orai1 and STIM1/2 transcript levels were even significantly lower than the transcript levels of untreated ChAc neurons (Fig. 1). Wogonin alone tended to decrease Orai1 transcript levels and significantly decreased STIM1/2 transcript levels (Fig. 1).

Western blotting was employed for quantification of protein abundance. As illustrated in Fig. 2, the Orai1 and STIM1 protein expressions were significantly higher in ChAc neurons following 24 hours incubation in the presence than in the absence of 2 mM lithium (Fig. 2). The additional treatment with the NFκB inhibitor wogonin (50 μM) significantly decreased the Orai1 and STIM1/2 protein abundance. In the presence of both, lithium and wogonin, the Orai1 and STIM1/2 protein abundances were not significantly different from the Orai1 and STIM1/2 protein abundances in the absence of lithium and wogonin (Fig. 2).

Altered expressions of Orai1 and STIM1 were expected to be paralleled by respective changes of store operated  $\text{Ca}^{2+}$  entry (SOCE). Fura2 fluorescence was thus employed to quantify the cytosolic  $\text{Ca}^{2+}$  concentration ( $[\text{Ca}^{2+}]_i$ ). For determination of SOCE, the intracellular stores were emptied by exposure of the cells to the sarco-/endoplasmic reticulum  $\text{Ca}^{2+}$ -ATPase (SERCA) inhibitor thapsigargin (1 μM) in the absence of extracellular  $\text{Ca}^{2+}$ . Re-addition of extracellular  $\text{Ca}^{2+}$  in the continued presence of thapsigargin resulted in a sharp increase of  $[\text{Ca}^{2+}]_i$  reflecting SOCE. As shown in Fig. 3B,C, emptying the intracellular  $\text{Ca}^{2+}$  stores with thapsigargin was followed by a transient increase in  $[\text{Ca}^{2+}]_i$ . The increase tended to be higher in lithium treated than in untreated ChAc neurons, a difference, however, not reaching statistical significance. The increase of  $[\text{Ca}^{2+}]_i$  following re-addition of extracellular  $\text{Ca}^{2+}$  in the continued presence of thapsigargin was significantly higher in lithium treated than in untreated ChAc neurons (Fig. 3D,E). Treatment with the NFκB inhibitor wogonin (50 μM) significantly decreased SOCE both, in the absence and presence of lithium. In the presence of both, lithium and wogonin, SOCE was significantly lower than in untreated ChAc neurons (Fig. 3D,E).

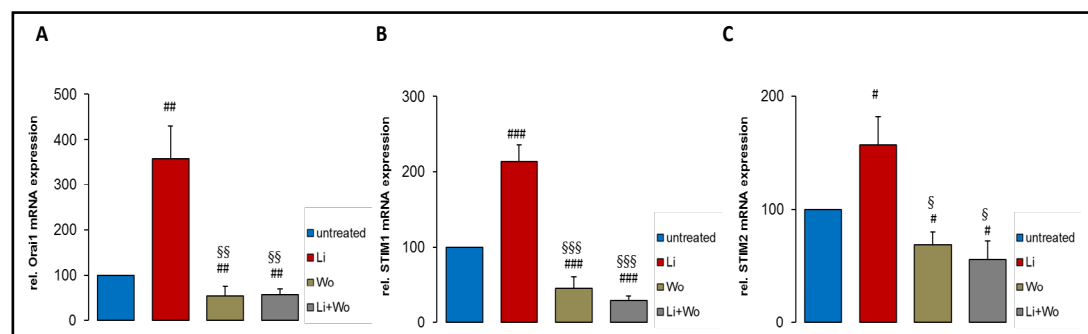


**Fig. 1.** Effect of lithium treatment with and without NFκB inhibitor wogonin on Orai1 STIM1 and STIM2 transcript levels in ChAc neurons. A,B,C. Arithmetic means ( $\pm$  SEM,  $n = 7$ ) of (A) Orai1, (B) STIM1, (C) STIM2 transcript levels in neurons generated from ChAc patients without (blue or yellow bars) or with (red and grey bars) lithium (24 h, 2 mM) treatment without (blue and red bars) and with (yellow and grey bars) presence of NFκB inhibitor wogonin (50 μM). ##( $p < 0.01$ ), ###( $p < 0.001$ ) indicates statistically significant difference to respective value in the absence of treatments, \$( $p < 0.05$ ), \$\$( $p < 0.01$ ), \$\$\$( $p < 0.001$ ) indicates statistically significant difference to respective value in the absence of wogonin.



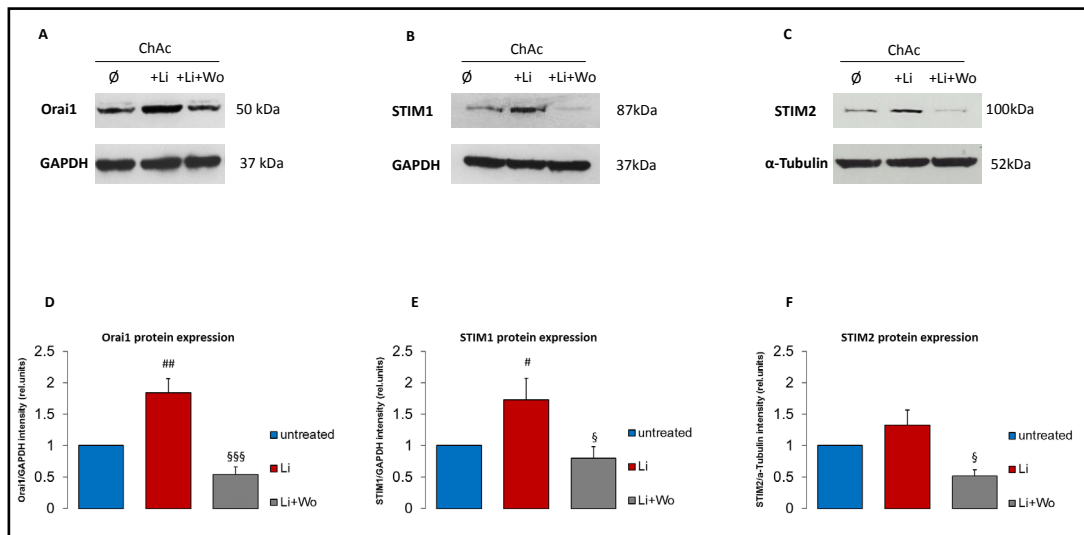


**Fig. 2.** Effect of lithium treatment without and with NFκB inhibitor wogonin on Orai1, STIM1 and STIM2 protein abundance in iPSC-derived neurons from ChAc patients. A,B,C. Original Western blot of (A) Orai1, (B) STIM1 and (C) STIM2 protein abundance in neurons differentiated from iPSCs derived from ChAc patients (ChAc) without or with lithium (24 h, 2 mM) treatment without and with presence of NFκB inhibitor wogonin (50 μM). D,E,F. Arithmetic means (± SEM, n = 5) of (D) Orai1, (E) STIM1 and (F) STIM2 protein abundance in neurons generated from iPSCs derived from ChAc patients without (blue bars) or with (red and grey bars) lithium (24 h, 2 mM) treatment without (red bars) and with (grey bars) presence of NFκB inhibitor wogonin (50 μM). # (p < 0.05), ## (p < 0.01) indicates statistically significant difference to respective value in the absence of treatment, § (p < 0.05), §§§ (p < 0.001) indicates statistically significant difference to respective value in the absence of wogonin.

The function of Orai1 was further quantified by measurement of  $\text{Ca}^{2+}$  release activated  $\text{Ca}^{2+}$  channel (CRAC) currents ( $I_{\text{CRAC}}$ ) utilizing whole cell patch clamp recording. As shown in Fig. 4,  $I_{\text{CRAC}}$  was significantly higher in lithium treated than in untreated ChAc neurons. The additional treatment with the NFκB inhibitor wogonin (50 μM) significantly decreased  $I_{\text{CRAC}}$  (Fig. 4).

## Discussion

The present study sheds further light on the signaling contributing to the regulation of Orai1, STIM1 and STIM2 expression,  $\text{Ca}^{2+}$  release activated channel (CRAC) currents ( $I_{\text{CRAC}}$ ) and store operated  $\text{Ca}^{2+}$  entry (SOCE) in chorea-acanthocytosis (ChAc) neurons. The results confirm the previous observations that lithium up-regulates Orai1 and STIM1 expression,  $I_{\text{CRAC}}$  and SOCE in ChAc neurons [27]. Inhibition of NFκB inhibitor wogonin abrogates the stimulating effect of lithium on Orai1 and STIM1/2 transcript levels and protein abundance, SOCE and CRAC current. Wogonin significantly decreases Orai1 and STIM1/2 transcript levels and SOCE even in the absence of lithium indicating that NFκB is stimulating Orai1 and STIM1/2 expression as well SOCE independent of lithium. NFκB may thus play a permissive role for the effect of lithium. In any case, NFκB is apparently a stimulator of Orai1 and STIM1/2 expression as well SOCE in both, the presence and absence of lithium.

Stimulation of SOCE may result in oscillations of cytosolic  $\text{Ca}^{2+}$  activity ( $[\text{Ca}^{2+}]_i$ ) [47] with rapid increase of  $[\text{Ca}^{2+}]_i$  due to intracellular  $\text{Ca}^{2+}$  release and activation of SOCE followed by rapid decrease of  $[\text{Ca}^{2+}]_i$  due to SOCE inhibition and  $\text{Ca}^{2+}$  extrusion [48]. The repeated short increases of  $[\text{Ca}^{2+}]_i$  are followed by activation of  $\text{Ca}^{2+}$  dependent transcription factors and reorganization of the actin filament network without cell injury resulting from sustained increases of  $[\text{Ca}^{2+}]_i$  [49, 50].

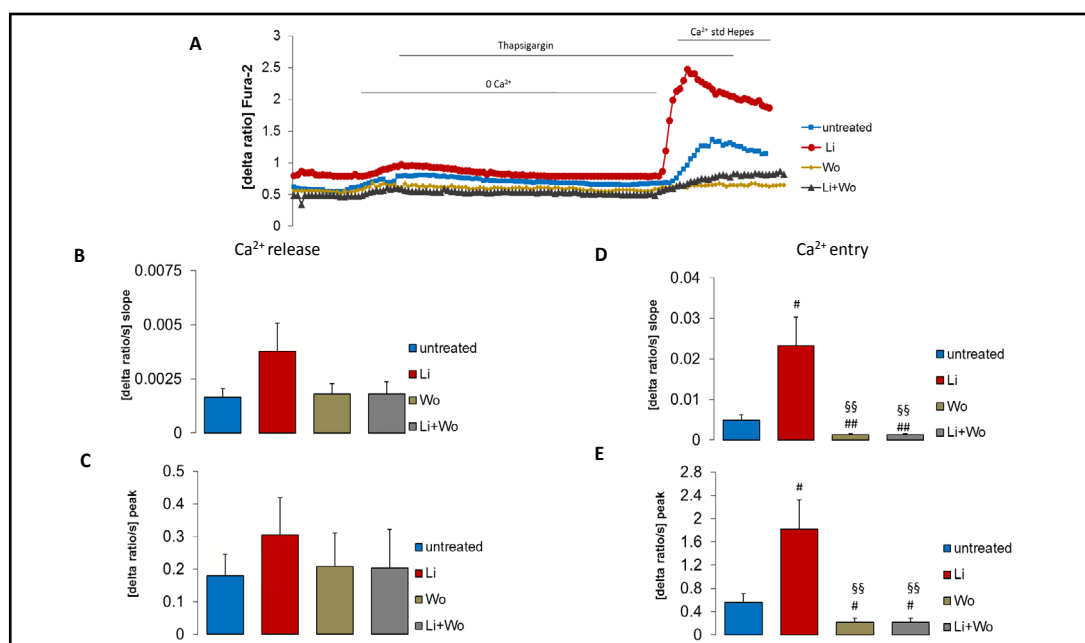
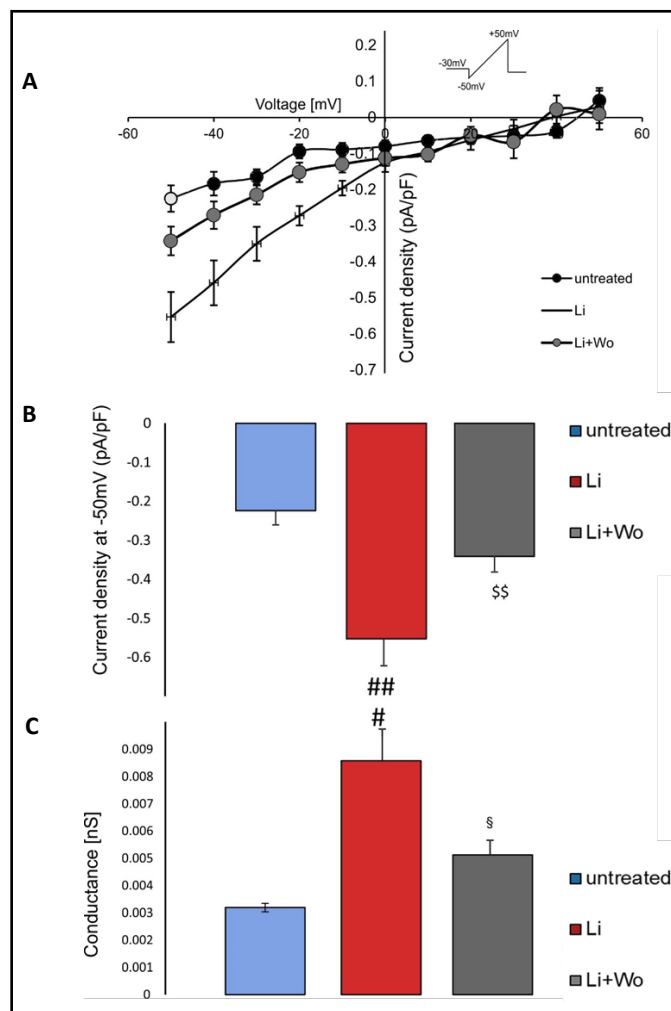


**Fig. 3.** Intracellular Ca<sup>2+</sup> release and store-operated Ca<sup>2+</sup> entry (SOCE) in iPSC-derived neurons from ChAc patients without or with lithium treatment without and with NFκB inhibitor wogonin. **A.** Representative tracings of Fura-2 fluorescence-ratio in fluorescence spectrometry before and following extracellular Ca<sup>2+</sup> removal and addition of thapsigargin (1 μM), as well as re-addition of extracellular Ca<sup>2+</sup> in neurons generated from ChAc patients without (blue) and with (red) lithium (24 h, 2 mM) treatment in the absence of NFκB inhibitor wogonin as well as without (yellow) and with (grey) lithium (24 h, 2 mM) in presence of NFκB inhibitor wogonin. **B,C.** Arithmetic means (± SEM, n = 30-40 cells from 3 individuals) of slope (**B**) and peak (**C**) increase of fura-2-fluorescence-ratio following addition of thapsigargin (1 μM) in ChAc neurons without (blue or yellow bars) or with (red and grey bars) lithium (24 h, 2 mM) treatment without (blue and red bars) and with (yellow and grey bars) NFκB inhibitor wogonin (50 μM). **D,E.** Arithmetic means (± SEM, n = 30-40 cells from 3 individuals) of slope (**D**) and peak (**E**) increase of fura-2-fluorescence-ratio following re-addition of extracellular Ca<sup>2+</sup> in neurons from ChAc patients without (blue or yellow bars) or with (red and grey bars) lithium (24 h, 2 mM) treatment without (blue and red bars) and with (yellow and grey bars) NFκB inhibitor wogonin (50 μM). # (p<0.05), ## (p<0.01) indicates statistically significant difference to respective value without treatment, §§ (p<0.01) indicates statistically significant difference to respective value in the absence of wogonin.

Ca<sup>2+</sup> oscillations trigger several cellular functions [51, 52] including entry into the S and the M phase of the cell cycle [53] and cell survival [54, 55]. The Orai isoforms [20] and their regulators STIM 1 or 2 [21] confer survival, proliferation, and migration of tumor cells [56-59] and neural stem/progenitor cells [60]. In contrast to Ca<sup>2+</sup> oscillations, sustained increases of cytosolic Ca<sup>2+</sup> activity trigger suicidal cell death [61-63].

Lithium has previously been shown to support survival of ChAc neurons [27]. Lithium has further been shown to favorably influence other neurodegenerative diseases including Huntington's chorea, Alzheimer's disease, Parkinson's disease, amyotrophic lateral sclerosis as well as spinocerebellar ataxias type 1 and type 3 [28-30, 64, 65]. Mechanisms invoked in the neuroprotective effect of lithium include direct or Akt-mediated inhibition of glycogen synthase kinase GSK-3β, Akt-mediated inhibition of the proapoptotic forkhead box class O transcription factor Foxo3a and murine double minute (MDM), stimulation of production and activity of neuroprotective brain derived neurotrophic factor BDNF, up-regulation of antiapoptotic protein Bcl-2, as well as down-regulation of proapoptotic transcription factor p53, of the proapoptotic proteins Bad and Bax, of glutamate excitotoxicity, of calpain and of oxidative stress [30, 66].

**Fig. 4.**  $\text{Ca}^{2+}$  release activated channel (CRAC) currents ( $I_{\text{CRAC}}$ ) in iPSC-derived neurons from ChAc patients without or with lithium treatment without and with NFκB inhibitor wogonin. **A.** Mean current-voltage (I/V) relationships of currents normalized to cell capacitance in neurons generated from ChAc patients without (n=7) or with lithium treatment without (n=6) and with (n=8) NFκB inhibitor wogonin. The voltage protocol is shown (not to scale), whereby cells were held at -30 mV and voltage steps were applied in 10 mV increments for 200 ms from -50 mV to +50 mV. **B.** Mean current density (normalized by capacitance) ( $\pm$  SEM, n=5-7) obtained from peak of current at -50 mV without (blue bars) or with lithium (24 h, 2 mM) treatment without (red bar) and with (grey bar) presence of NFκB inhibitor wogonin (50  $\mu\text{M}$ ). **C.** Mean whole-cell conductance of inward currents ( $\pm$  SEM, n=5-7) calculated by linear regression of I/V curves shown in (A) between -50 mV and -10 mV without (blue bars) or with lithium (24 h, 2 mM) treatment without (red bars) and with (grey bars) presence of NFκB inhibitor wogonin (50  $\mu\text{M}$ ). ##(p<0.01), ###(p<0.001) indicates statistically significant difference to respective value in the absence of lithium treatment. #(p<0.05), ##(p<0.01) indicates statistically significant difference to respective value in untreated cells, \$(p<0.05) indicates statistically significant difference to respective value in the absence of wogonin.



The stimulating effect of NFκB on Orai1/STIM1 expression,  $I_{\text{CRAC}}$  and SOCE observed here could, at least in theory, impact on neuronal cell survival and contribute to the beneficial effect of lithium. The present observations, however, cannot be taken as evidence for an inhibitory effect of NFκB on neurodegeneration. NFκB expressed in microglial cells has previously been shown to participate in the orchestration of neuroinflammation and thus neurodegeneration [67-69] and NF-κB inhibitors are considered as potential treatment for neurodegenerative diseases [69]. It should be further kept in mind that neurons gained by reprogramming of skin fibroblasts and kept in cell culture do not necessarily respond to challenges in an identical way as neurons in situ. Thus, caution is warranted if the present results are extrapolated to native human physiology and pathophysiology.

## Conclusion

In conclusion, pharmacological inhibition of NFκB markedly decreases Orai1 and STIM1 expression as well as  $I_{\text{CRAC}}$  and store operated  $\text{Ca}^{2+}$  entry in cultured ChAc neurons. It further abrogates the stimulating effect of lithium on Orai1 and STIM1 expression as well as  $I_{\text{CRAC}}$  and



store operated  $\text{Ca}^{2+}$  entry in ChAc neurons. To which extent this effect impacts on ChAc and other neurodegenerative disorders, remains to be shown.

## Acknowledgements

The authors acknowledge the meticulous preparation of the manuscript by Lejla Subasic and the technical support by Yvonne Schelling. This work was supported by grants from Brigitte-Schlieben-Lange-Programm to L.P. by the Deutscher Akademischer Austauschdienst (DAAD) bi-nationally supervised Ph.D. Fellowship to I.S., by the Deutsche Forschungsgemeinschaft (La315-15) to F.L. and by the Open Access Publishing Fund, University of Tuebingen.

B.S., S.H., L.P., Z.H., I.S., T.M., A.M. performed experiments, C.S., L.S., F.L. designed the study and share last authorship for this paper, and F.L. drafted the manuscript. All authors corrected and approved the final version of the manuscript.

## Disclosure Statement

The sponsors had no role in study design, the collection, analysis and interpretation of data, in the writing of the report, and in the decision to submit the article for publication. All authors confirm that they have no competing financial interests to disclose.

## References

- 1 IntAct Dfif: [<http://www.ebi.ac.uk/intact/pages/interactions/interactions.xhtml?conversationContext=1>]. EMBL EBI database 2011.
- 2 Foller M, Hermann A, Gu S, Alesutan I, Qadri SM, Borst O, Schmidt EM, Schiele F, vom Hagen JM, Saft C, Schols L, Lerche H, Stournaras C, Storch A, Lang F: Chorein-sensitive polymerization of cortical actin and suicidal cell death in chorea-acanthocytosis. *FASEB J* 2012;26:1526-1534.
- 3 Honisch S, Yu W, Liu G, Alesutan I, Towhid ST, Tsapara A, Schleicher S, Handgretinger R, Stournaras C, Lang F: Chorein addiction in VPS13A overexpressing rhabdomyosarcoma cells. *Oncotarget* 2015;6:10309-10319.
- 4 Lang F, Pelzl L, Schols L, Hermann A, Foller M, Schaffer TE, Stournaras C: Neurons, Erythrocytes and Beyond -The Diverse Functions of Chorein. *Neurosignals* 2017;25:117-126.
- 5 Dobson-Stone C, Rampoldi L, Bader B, Velayos BA, Walker RH, Danek A, Monaco AP: Choreia-Acanthocytosis. *Gene Rev* 1993;updated 2010.
- 6 Ueno S, Maruki Y, Nakamura M, Tomemori Y, Kamae K, Tanabe H, Yamashita Y, Matsuda S, Kaneko S, Sano A: The gene encoding a newly discovered protein, chorein, is mutated in chorea-acanthocytosis. *Nat Genet* 2001;28:121-122.
- 7 Dobson-Stone C, Danek A, Rampoldi L, Hardie RJ, Chalmers RM, Wood NW, Bohlega S, Dotti MT, Federico A, Shizuka M, Tanaka M, Watanabe M, Ikeda Y, Brin M, Goldfarb LG, Karp BI, Mohiddin S, Fananapazir L, Storch A, Fryer AE et al.: Mutational spectrum of the CHAC gene in patients with chorea-acanthocytosis. *Eur J Hum Genet* 2002;10:773-781.
- 8 Saiki S, Sakai K, Murata KY, Saiki M, Nakanishi M, Kitagawa Y, Kaito M, Gondo Y, Kumamoto T, Matsui M, Hattori N, Hirose G: Primary skeletal muscle involvement in chorea-acanthocytosis. *Mov Disord* 2007;22:848-852.
- 9 Velayos Baeza A, Dobson-Stone C, Rampoldi L, Bader B, Walker RH, Danek A, Monaco AP: Choreia-Acanthocytosis; in (Pagon RA, Adam MP, Ardinger HH, Wallace SE, Amemiya A, Bean LJH, Bird TD, Ledbetter N, Mefford HC, Smith RJH, and Stephens K, eds) *GeneReviews*(R). Seattle (WA), University of Washington, Seattle. GeneReviews is a registered trademark of the University of Washington, Seattle. All rights reserved., 1993, vol. p.^pp.

- 10 Walterfang M, Looi JC, Styner M, Walker RH, Danek A, Niethammer M, Evans A, Kotschet K, Rodrigues GR, Hughes A, Velakoulis D: Shape alterations in the striatum in chorea-acanthocytosis. *Psychiatry Res* 2011;192:29-36.
- 11 Tomemori Y, Ichiba M, Kusumoto A, Mizuno E, Sato D, Muroya S, Nakamura M, Kawaguchi H, Yoshida H, Ueno S, Nakao K, Nakamura K, Aiba A, Katsuki M, Sano A: A gene-targeted mouse model for chorea-acanthocytosis. *J Neurochem* 2005;92:759-766.
- 12 Kurano Y, Nakamura M, Ichiba M, Matsuda M, Mizuno E, Kato M, Agemura A, Izumo S, Sano A: *In vivo* distribution and localization of chorein. *Biochem Biophys Res Commun* 2007;353:431-435.
- 13 Alesutan I, Seifert J, Pakladok T, Rheinlaender J, Lebedeva A, Towhid ST, Stournaras C, Voelkl J, Schaffer TE, Lang F: Chorein sensitivity of actin polymerization, cell shape and mechanical stiffness of vascular endothelial cells. *Cell Physiol Biochem* 2013;32:728-742.
- 14 Schmidt EM, Schmid E, Munzer P, Hermann A, Eyrych AK, Russo A, Walker B, Gu S, vom Hagen JM, Faggio C, Schaller M, Foller M, Schols L, Gawaz M, Borst O, Storch A, Stournaras C, Lang F: Chorein sensitivity of cytoskeletal organization and degranulation of platelets. *FASEB J* 2013;27:2799-2806.
- 15 Honisch S, Fehrenbacher B, Lebedeva A, Alesutan I, Castor T, Alkahtani S, Alarifi S, Schaller M, Stournaras C, Lang F: Chorein Sensitive Dopamine Release from Pheochromocytoma (PC12) Cells. *Neurosignals* 2015;23:1-10.
- 16 Honisch S, Gu S, Vom Hagen JM, Alkahtani S, Al Kahtane AA, Tsapara A, Hermann A, Storch A, Schols L, Lang F, Stournaras C: Chorein Sensitive Arrangement of Cytoskeletal Architecture. *Cell Physiol Biochem* 2015;37:399-408.
- 17 Saiki S, Sakai K, Murata KY, Saiki M, Nakanishi M, Kitagawa Y, Kaito M, Gondo Y, Kumamoto T, Matsui M, Hattori N, Hirose G: Primary skeletal muscle involvement in chorea-acanthocytosis. *Mov Disord* 2007;22:848-852.
- 18 Orrenius S, Zhivotovsky B, Nicotera P: Regulation of cell death: the calcium-apoptosis link. *Nat Rev Mol Cell Biol* 2003;4:552-565.
- 19 Burgoyne RD: Neuronal calcium sensor proteins: generating diversity in neuronal Ca<sup>2+</sup> signalling. *Nat Rev Neurosci* 2007;8:182-193.
- 20 Putney JW, Jr.: New molecular players in capacitative Ca<sup>2+</sup> entry. *J Cell Sci* 2007;120:1959-1965.
- 21 Peinelt C, Vig M, Koomoa DL, Beck A, Nadler MJ, Koblan-Huberson M, Lis A, Fleig A, Penner R, Kinet JP: Amplification of CRAC current by STIM1 and CRACM1 (Orai1). *Nat Cell Biol* 2006;8:771-773.
- 22 Smyth JT, Hwang SY, Tomita T, DeHaven WI, Mercer JC, Putney JW: Activation and regulation of store-operated calcium entry. *J Cell Mol Med* 2010;14:2337-2349.
- 23 Penna A, Demuro A, Yeromin AV, Zhang SL, Safrina O, Parker I, Cahalan MD: The CRAC channel consists of a tetramer formed by Stim-induced dimerization of Orai dimers. *Nature* 2008;456:116-120.
- 24 Yu W, Honisch S, Schmidt S, Yan J, Schmid E, Alkahtani S, Alkahtane AA, Alarifi S, Stournaras C, Lang F: Chorein Sensitive Orai1 Expression and Store Operated Ca<sup>2+</sup> Entry in Rhabdomyosarcoma Cells. *Cell Physiol Biochem* 2016;40:1141-1152.
- 25 Zhang B, Yan J, Schmidt S, Salkner MS, Alexander D, Foller M, Lang F: Lithium- Sensitive Store-Operated Ca<sup>2+</sup> Entry in the Regulation of FGF23 Release. *Neurosignals* 2015;23:34-48.
- 26 Pelzl L, Elsir B, Sahu I, Bissinger R, Singh Y, Sukkar B, Honisch S, Schoels L, Jemaa M, Lang E, Storch A, Hermann A, Stournaras C, Lang F: Lithium Sensitivity of Store Operated Ca<sup>2+</sup> Entry and Survival of Fibroblasts Isolated from Chorea-Acanthocytosis Patients. *Cell Physiol Biochem* 2017;42:2066-2077.
- 27 Pelzl L, Hauser S, Elsir B, Sukkar B, Sahu I, Singh Y, Hoflinger P, Bissinger R, Jemaa M, Stournaras C, Schols L, Lang F: Lithium Sensitive ORAI1 Expression, Store Operated Ca(2+) Entry and Suicidal Death of Neurons in Chorea-Acanthocytosis. *Sci Rep* 2017;7:6457.
- 28 Alvarez G, Munoz-Montano JR, Satrustegui J, Avila J, Bogonez E, Diaz-Nido J: Regulation of tau phosphorylation and protection against beta-amyloid-induced neurodegeneration by lithium. Possible implications for Alzheimer's disease. *Bipolar Disord* 2002;4:153-165.
- 29 Bauer M, Alda M, Priller J, Young LT, International Group For The Study Of Lithium Treated P: Implications of the neuroprotective effects of lithium for the treatment of bipolar and neurodegenerative disorders. *Pharmacopsychiatry* 2003;36 Suppl 3:S250-254.
- 30 Lazzara CA, Kim YH: Potential application of lithium in Parkinson's and other neurodegenerative diseases. *Front Neurosci* 2015;9:403.

- 31 Lang F, Eylonstein A, Shumilina E: Regulation of Orai1/STIM1 by the kinases SGK1 and AMPK. *Cell Calcium* 2012;52:347-354.
- 32 Schmidt S, Liu G, Liu G, Yang W, Honisch S, Pantelakos S, Stournaras C, Honig A, Lang F: Enhanced Orai1 and STIM1 expression as well as store operated Ca<sup>2+</sup> entry in therapy resistant ovary carcinoma cells. *Oncotarget* 2014;5:4799-4810.
- 33 Fruman DA, Rommel C: PI3K and cancer: lessons, challenges and opportunities. *Nat Rev Drug Discov* 2014;13:140-156.
- 34 Ocana A, Vera-Badillo F, Al-Mubarak M, Templeton AJ, Corrales-Sanchez V, Diez-Gonzalez L, Cuenca-Lopez MD, Seruga B, Pandiella A, Amir E: Activation of the PI3K/mTOR/AKT pathway and survival in solid tumors: systematic review and meta-analysis. *PLoS One* 2014;9:e95219.
- 35 Rodon J, Dienstmann R, Serra V, Tabernero J: Development of PI3K inhibitors: lessons learned from early clinical trials. *Nat Rev Clin Oncol* 2013;10:143-153.
- 36 Zhang L, Zhou F, ten Dijke P: Signaling interplay between transforming growth factor-beta receptor and PI3K/AKT pathways in cancer. *Trends Biochem Sci* 2013;38:612-620.
- 37 Sedding DG: FoxO transcription factors in oxidative stress response and ageing--a new fork on the way to longevity? *Biol Chem* 2008;389:279-283.
- 38 Dudek H, Datta SR, Franke TF, Birnbaum MJ, Yao R, Cooper GM, Segal RA, Kaplan DR, Greenberg ME: Regulation of neuronal survival by the serine-threonine protein kinase Akt. *Science* 1997;275:661-665.
- 39 Arboleda G, Morales LC, Benitez B, Arboleda H: Regulation of ceramide-induced neuronal death: cell metabolism meets neurodegeneration. *Brain Res Rev* 2009;59:333-346.
- 40 Kreis P, Rousseau V, Thevenot E, Combeau G, Barnier JV: The four mammalian splice variants encoded by the p21-activated kinase 3 gene have different biological properties. *J Neurochem* 2008;106:1184-1197.
- 41 Okita K, Matsumura Y, Sato Y, Okada A, Morizane A, Okamoto S, Hong H, Nakagawa M, Tanabe K, Tezuka K, Shibata T, Kunisada T, Takahashi M, Takahashi J, Saji H, Yamanaka S: A more efficient method to generate integration-free human iPS cells. *Nat Methods* 2011;8:409-412.
- 42 Hauser S, Hoflinger P, Theurer Y, Rattay TW, Schols L: Generation of induced pluripotent stem cells (iPSCs) from a hereditary spastic paraplegia patient carrying a homozygous Y275X mutation in CYP7B1 (SPG5). *Stem Cell Res* 2016;17:437-440.
- 43 Ichida JK, Kiskinis E: Probing disorders of the nervous system using reprogramming approaches. *EMBO J* 2015;34:1456-1477.
- 44 Shi Y, Kirwan P, Livesey FJ: Directed differentiation of human pluripotent stem cells to cerebral cortex neurons and neural networks. *Nat Protoc* 2012;7:1836-1846.
- 45 Jiang P, Bian M, Ma W, Liu C, Yang P, Zhu B, Xu Y, Zheng M, Qiao J, Shuai Z, Zhou X, Huang D: Eryptosis as an Underlying Mechanism in Systemic Lupus Erythematosus-Related Anemia. *Cell Physiol Biochem* 2016;40:1391-1400.
- 46 Yan J, Zhang B, Hosseinzadeh Z, Lang F: Down-Regulation of Store-Operated Ca<sup>2+</sup> Entry and Na<sup>+</sup> Ca<sup>2+</sup> Exchange in MCF-7 Breast Cancer Cells by Pharmacological JAK3 Inhibition. *Cell Physiol Biochem* 2016;38:1643-1651.
- 47 Lang F, Friedrich F, Kahn E, Woll E, Hammerer M, Waldegger S, Maly K, Grunicke H: Bradykinin-induced oscillations of cell membrane potential in cells expressing the Ha-ras oncogene. *J Biol Chem* 1991;266:4938-4942.
- 48 Parekh AB: Regulation of CRAC channels by Ca<sup>2+</sup>-dependent inactivation. *Cell Calcium* 2016;10.1016/j.ceca.2016.12.003
- 49 Lang F, Shumilina E, Ritter M, Gulbins E, Vereninov A, Huber SM: Ion channels and cell volume in regulation of cell proliferation and apoptotic cell death. *Contrib Nephrol* 2006;152:142-160.
- 50 Lang F, Stournaras C: Ion channels in cancer: future perspectives and clinical potential. *Philos Trans R Soc Lond B Biol Sci* 2014;369:20130108.
- 51 Berridge MJ, Bootman MD, Roderick HL: Calcium signalling: dynamics, homeostasis and remodelling. *Nat Rev Mol Cell Biol* 2003;4:517-529.
- 52 Parekh AB, Penner R: Store depletion and calcium influx. *Physiol Rev* 1997;77:901-930.
- 53 Taylor JT, Zeng XB, Pottle JE, Lee K, Wang AR, Yi SG, Scruggs JA, Sikka SS, Li M: Calcium signaling and T-type calcium channels in cancer cell cycling. *World J Gastroenterol* 2008;14:4984-4991.

- 54 Heise N, Palme D, Misovic M, Koka S, Rudner J, Lang F, Salih HR, Huber SM, Henke G: Non-selective cation channel-mediated Ca<sup>2+</sup>-entry and activation of Ca<sup>2+</sup>/calmodulin-dependent kinase II contribute to G2/M cell cycle arrest and survival of irradiated leukemia cells. *Cell Physiol Biochem* 2010;26:597-608.
- 55 Parkash J, Asotra K: Calcium wave signaling in cancer cells. *Life Sci* 2010;87:587-595.
- 56 Bergmeier W, Weidinger C, Zee I, Feske S: Emerging roles of store-operated Ca<sup>2</sup>(+ entry through STIM and ORAI proteins in immunity, hemostasis and cancer. *Channels (Austin)* 2013;7:379-391.
- 57 Prevarskaya N, Skryma R, Shuba Y: Calcium in tumour metastasis: new roles for known actors. *Nat Rev Cancer* 2011;11:609-618.
- 58 Prevarskaya N, Ouadid-Ahidouch H, Skryma R, Shuba Y: Remodelling of Ca<sup>2+</sup> transport in cancer: how it contributes to cancer hallmarks? *Philos Trans R Soc Lond B Biol Sci* 2014;369:20130097.
- 59 Qu B, Al-Ansary D, Kummerow C, Hoth M, Schwarz EC: ORAI-mediated calcium influx in T cell proliferation, apoptosis and tolerance. *Cell Calcium* 2011;50:261-269.
- 60 Somasundaram A, Shum AK, McBride HJ, Kessler JA, Feske S, Miller RJ, Prakriya M: Store-operated CRAC channels regulate gene expression and proliferation in neural progenitor cells. *J Neurosci* 2014;34:9107-9123.
- 61 Fang KM, Chang WL, Wang SM, Su MJ, Wu ML: Arachidonic acid induces both Na<sup>+</sup> and Ca<sup>2+</sup> entry resulting in apoptosis. *J Neurochem* 2008;104:1177-1189.
- 62 Lang F, Hoffmann EK: Role of ion transport in control of apoptotic cell death. *Compr Physiol* 2012;2:2037-2061.
- 63 Green DR, Reed JC: Mitochondria and apoptosis. *Science* 1998;281:1309-1312.
- 64 Jia DD, Zhang L, Chen Z, Wang CR, Huang FZ, Duan RH, Xia K, Tang BS, Jiang H: Lithium chloride alleviates neurodegeneration partly by inhibiting activity of GSK3β in a SCA3 Drosophila model. *Cerebellum* 2013;12:892-901.
- 65 Watase K, Gatchel JR, Sun Y, Emamian E, Atkinson R, Richman R, Mizusawa H, Orr HT, Shaw C, Zoghbi HY: Lithium therapy improves neurological function and hippocampal dendritic arborization in a spinocerebellar ataxia type 1 mouse model. *PLoS Med* 2007;4:e182.
- 66 Mao Z, Liu L, Zhang R, Li X: Lithium reduces FoxO3a transcriptional activity by decreasing its intracellular content. *Biol Psychiatry* 2007;62:1423-1430.
- 67 Kopitar-Jerala N: Innate Immune Response in Brain, NF-Kappa B Signaling and Cystatins. *Front Mol Neurosci* 2015;8:73.
- 68 Wardyn JD, Ponsford AH, Sanderson CM: Dissecting molecular cross-talk between Nrf2 and NF-kappaB response pathways. *Biochem Soc Trans* 2015;43:621-626.
- 69 Srinivasan M, Lahiri DK: Significance of NF-kappaB as a pivotal therapeutic target in the neurodegenerative pathologies of Alzheimer's disease and multiple sclerosis. *Expert Opin Ther Targets* 2015;19:471-487.